

Electronic Supplementary information (ESI) for

**Heterogeneous Junction Engineering on Core-Shell Nanocatalysts Boost the
Dye-Sensitized Solar Cell**

Authors: **Chiun-Yi Wu**,^a Yu-Ting Liu,^b Po-Chun Huang,^a Tzy-Jiun Mark Luo,^c
Chih-Hao Lee,^{a,d} Yaw-Wen Yang,^d Ten-Chin Wen,^e Tsan-Yao Chen,^{*a} and Tsang-Lang
Lin^{*a}

Affiliations:

^a. Department of Engineering and System Science, National Tsing Hua University,
Hsinchu 30013, Taiwan

^b. Department of Environmental Engineering, Tunghai University, Taichung, Taiwan

^c. Department of Materials Science and Engineering, North Carolina State University,
Raleigh, NC 27695, USA

^d. National Synchrotron Radiation Research Center, Hsinchu 30076, Taiwan

^e. Department of Chemical Engineering, National Cheng Kung University, Tainan
70001, Taiwan

*To whom correspondence should be addressed: Tsan-Yao Chen, email:
chencaeser@gmail.com; and Tsang-Lang Lin, email: tlilin@mx.nthu.edu.tw Tel:
+886-3-5742671 (O); +886-3-5728445 (Fax)

23

24 1. Synthetic procedure of Co–Pt core–shell CNCs and the preparation of CNCs/FTO
25 cathode.

26 The synthesis of $\text{Co}_{\text{core}}\text{-Pt}_{\text{shell}}$ NCs (denoted as Pt_s/Co_c) with a precisely controlled
27 thickness around 1.5 atomic layers was conducted by combining chemical reduction
28 and poylol reaction. In the first step, cobalt core NPs was grown by wet chemical
29 reduction method. It was conducted by adding 10 ml of 300 mM sodium borohydride
30 $[\text{NaBH}_4]$ water solution into 40 grams of 20 mM cobalt acetate tetrahydrate
31 $[\text{C}_4\text{H}_6\text{CoO}_4 \cdot 4\text{H}_2\text{O}]$ ethylene glycol (EG) solution in a presence of 10 wt% of
32 polyvinylpyrrolidone stabilizer (PVP-40, MW = 40 k). The solution of PVP blended
33 Co NPs (Co-PVP) was re-dispersed in EG into a metal contain of 10 mM and then
34 heated to 160°C to dehydrate for 2 h. After dehydration and cooling to room
35 temperature, the Pt shell crystal was grown by mixing Co-PVP with
36 hexachloroplatinic acid $[\text{H}_2\text{PtCl}_6 \cdot 6\text{H}_2\text{O}]$ then treated at 160°C for another 2 h. The Pt
37 shell thickness was adjusted by changing the Pt/Co ratio. The entire procedure was
38 conducted under an ambient atmosphere. After the NPs were synthesized, the entire
39 solution (sample) was mixed with 9 times or high of acetone solvent. This procedure
40 will induce the condensation of polymer blended NPs from the product. These NPs
41 was then redispersed into adequate amount of ethanol to form the slurry. The cathode
42 was prepared by spin coating the slurry onto FTO glass followed by the annealing at
43 300°C for 30 min (see Figure S1).

44

2. DSSC assembling procedure

The anode and cathode of DSSC were synthesized by coating the slurries of commercial ~25 nm titanium oxide powder paste and polymer blended Co-Pt core-shell nanoparticle on the FTO glass, respectively. The resulting anode is a porous ~21 – 22 nm thick P25@FTO thin-film. It was annealed at 450°C for 30 min, cooled down to room temperature, and then immersed into the TiO₂ precursor (50 mM TiCl₄/EtOH). The immersion improves the packing density (roughness factor) and thus increasing the specific number density of arched dye on anode for harvesting sun radiation. After immersion, the anode was annealed and then immersed into the dye solution for 24h. The spacer was made by a ~80 µm thick surlyn thin film with the flow channel patterns. The DSSC module was assembled by hot pressing the P25/FTO anode, the patterned surlyn, and the NPs/FTO cathode at 80°C for 5 min. As shown in the Figure S1, the electrolyte was injected into the DSSC channel by syringe pump for the PV measurement.

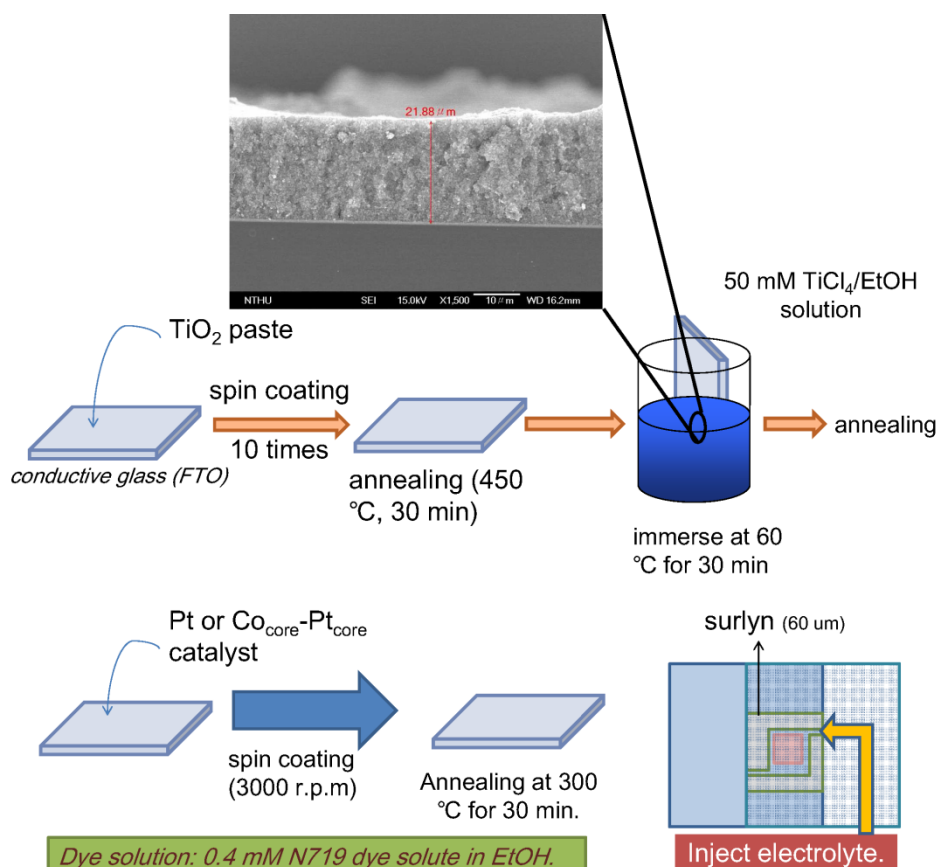
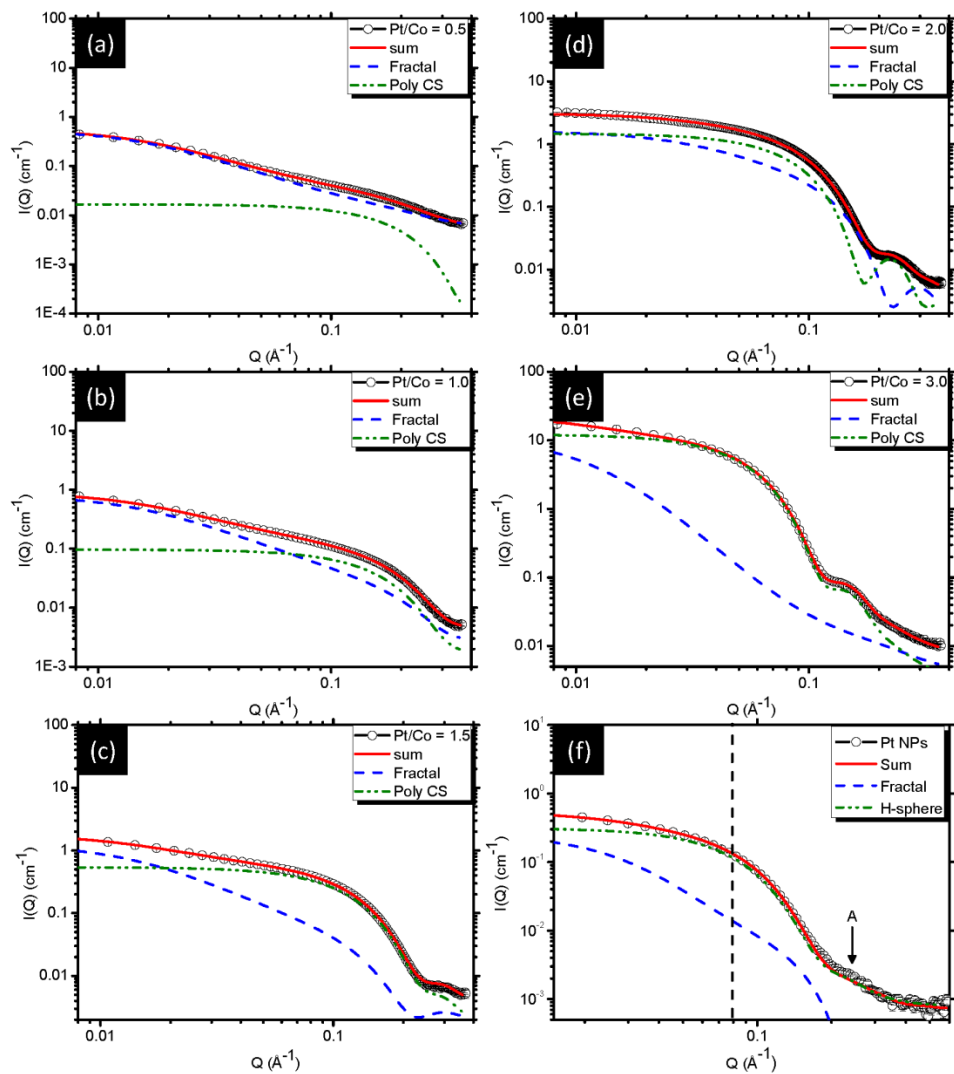


Figure S1. Schematic representation for the fabrication of NPs coated cathode and anode in a DSSC module.

65 3. SAXS characterization



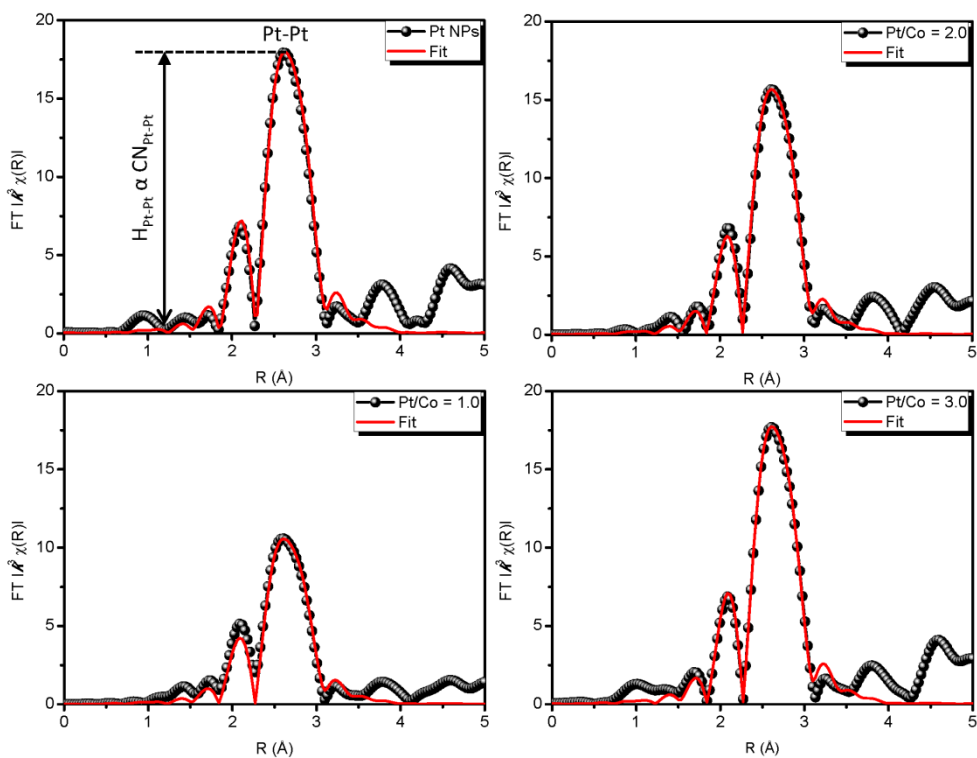
66
67 Figure S2: SAXS spectra with fitting Curve of Co-Pt core-shell NPs. Model labels,
68 Poly CS: polydispersed core-shell particle model; Fractal: fractal aggregation,
69 H-sphere: hard sphere with Shultz distribution of particle size.

73 Table S1 SAXS determined structure parameters of core-shell NPs.

NPs	Structure parameters						Applied fitting model
	D_F	Interparticle*	Intraparticle**				
		R_B (Å)	ξ (Å)	W/D_{all} (%)	D_C (Å)	T_S (Å)	
Pt/Co = 0.5	1.78	9.55	61.65	9.9	10.8	2.12	Fractal + poly CS
Pt/Co = 1.0	1.75	11.87	65.49	8.9	10.46	2.35	
Pt/Co = 1.5	1.95	18.52	67.31	8.9	15.78	4.11	
Pt/Co = 2.0	1.95	19.39	62.72	9.1	17.02	9.23	
Pt/Co = 3.0	2.51	8.15	75.61	15.0	24.10	23.93	
Pt NPs***	3.04	18.15	25.93	27.1	41.91	NA	Fractal + H-sphere

74 * D_F : fractal dimension (particle packing dimension), R_B : bulk radius (radius of
75 individual particle in a fractal aggregate), ξ : coherent length (dimension of a fractal
76 aggregate), W/D_{all} : polydispersity of particle size
77 ** D_C : dimension of core crystallite
78 *** D_C for Pt NPs refer to the average particle (D_{avg})
79

80 4. XAS characterization



81

82 Figure S3. Pt L_3 -edge Fourier transformed EXAFS spectra with the fitting curves for
83 CNCs of (a) Pt NPs and C/P CNCs of the Pt/Co ratios of (a) 1.0, (b) 2.0, and (c) 3.0,
84 respectively.

85

86 Table S2. Pt L_3 -edge XAS determined structure parameters of Pt NPs and C/P CNCs
87 of different Pt/Co ratios.

CNCs	Bond pair	R (Å)	CN^*
PtNPs	Pt-Pt	2.765	9.5
Pt/Co = 1.0	Pt-Pt	2.749	5.5
Pt/Co = 2.0	Pt-Pt	2.751	8.2
Pt/Co = 3.0	Pt-Pt	2.751	9.2

88

*coordination number

89

90 The extent of Co oxidation on C/P CNCs was determined by Co K-edge XAS
91 analysis including the X-ray absorption near edge structure (XANES) and extended
92 X-ray absorption fine structure (EXAFS). The normalized Co K-edge XANES
93 structure at room temperature for C/P CNCs of different Pt/Co ratios is shown in Fig.
94 S4a. The energy is calibrated by using a Co metal foil with threshold energy of $E_0 =$
95 7709 eV at the inflection point of the edge (region A, 1s-4d transition). The E_0 for the

standard Coacac (Co 3+) indicates a substantial shift of the edge energy with increasing Pt/Co ratio. The almost identical threshold edge energy E_0 at 7720 eV for the C/P CNCs indicates that all samples are very close to the stoichiometric composition with trivalent Co³⁺. The *K*-edge XANES main edge absorption is attributed to the 1s-4p dipole transition to the Co 4p states. The *K*-edge XANES main edge absorption is attributed to the 1s-4p dipole transition to the Co 4p states. The main edge features, labeled as B, C, and D, can be reasonably explained by the Co 4p partial density of states, their broadening reflects the finite lifetime of the 1s core hole [I. S. Elmov, V. I. Anisimov, and G. A. Sawatzky, Phys. Rev. Lett. 82, 4264 (1999)]. Feature B is attributed to the hybridization between the Co 4p states with the neighboring Pt 5d orbitals, C 2s, and O 2p, feature C is the Co 4p states split by the crystal field. Here, the increased feature C intensity suggesting that the strengthened heteroatomic orbital coupling at Co with neighboring atoms (i.e., C and O atoms). This coupling goes maximum extent due to the substantial Pt-to-Co transmetalation by increasing the Pt/Co ratio to 2.0. In this case, a considerable amount of Co atoms is transformed into metallic complex and then interacts with the CHO: radicals during polyol reduction. It triggers to the heterogeneous nucleation - growth pathways to form the heteroatomic Pt_(1-x)Co_x alloys at the CNCs surface ($x \ll 1$) and results in a certain amount of retained Co-complex. The surface Co atoms and retained Co-complexes will be stabilized by pyridine ligands and thus resulting in the Co carbide and oxides during the subsequent annealing. Further increasing the Pt/Co ratio to 3.0 suppresses the coupling of between Co and neighboring O atoms. This is due to the embedment of Co atoms by certain extent in the rapidly grown Pt shell.

The suppression of Co-O bondings by increasing Pt shell (Co embedment) can be further revealed by the EXAFS analysis. The radial structure function curves of C/P CNCs of different Pt/Co ratios with the corresponding model simulation curves are compared in Figure S4b, S4c, and S4d. As indicated, the radial peak at ~1.6 Å refers to the interferences of first nearest shell (R^{1st}) bond pairs of Co atom. The simulation curves of bond pairs are presented, which indicating that the 1st radial peak is originated from the combination of Co-O (A) and Co-O (B, C, and D) bonds in the crystalline Co carbide phase (Co₃O₄) and the Co-C^C, respectively. Quantitative structure parameters are given by the model simulation and results are summarized in the Table S3. As clearly can be seen, the coordination number of Pt-C bond pair “CN(Pt-C)” is increased with the Pt/Co ratios which consistent with the XRD results suggesting the growth of Co-C^C crystalline. On the other hand, the decreasing of peak A intensity (i.e., CN(Pt-O)) could be rationalized by the embedment of Co atoms by growing the Pt shell crystalline.

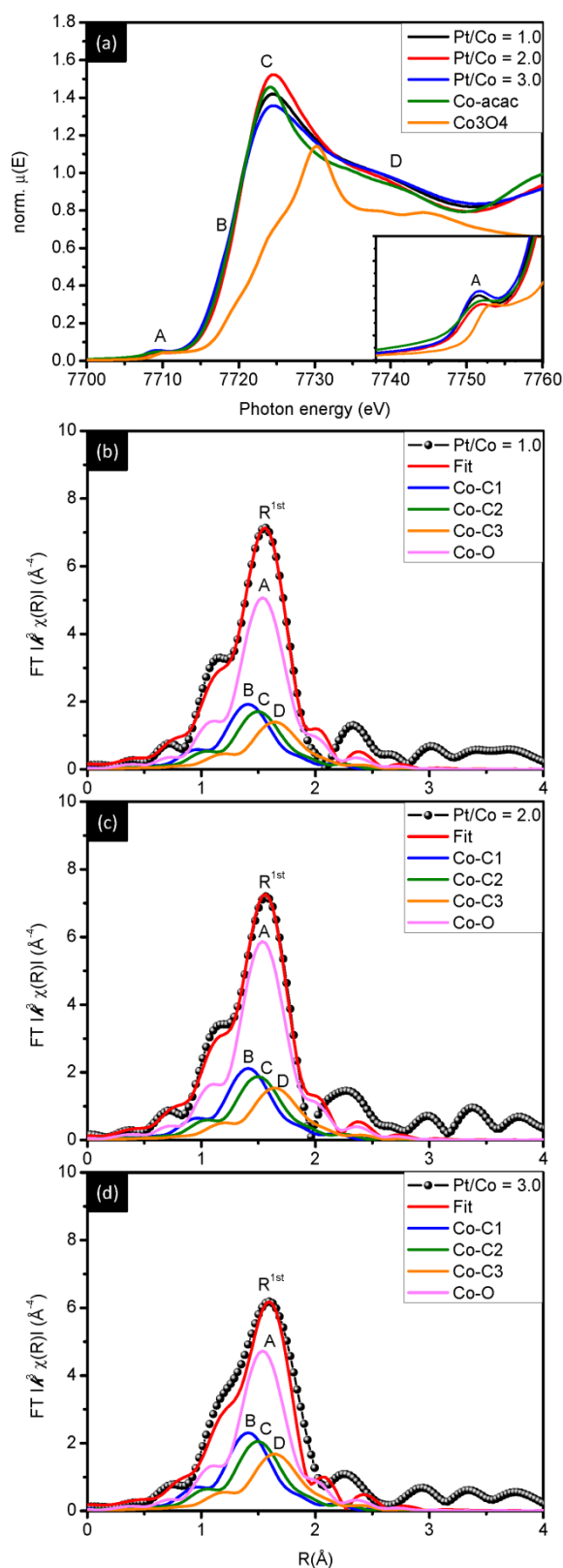


Figure S4. (a) XANES spectra of C/P CNCs of different Pt/Co ratios and Radial structure functions of C/P CNCs with the Pt/Co ratios of (b) 1.0, (c) 2.0, and (d) 3.0, respectively.

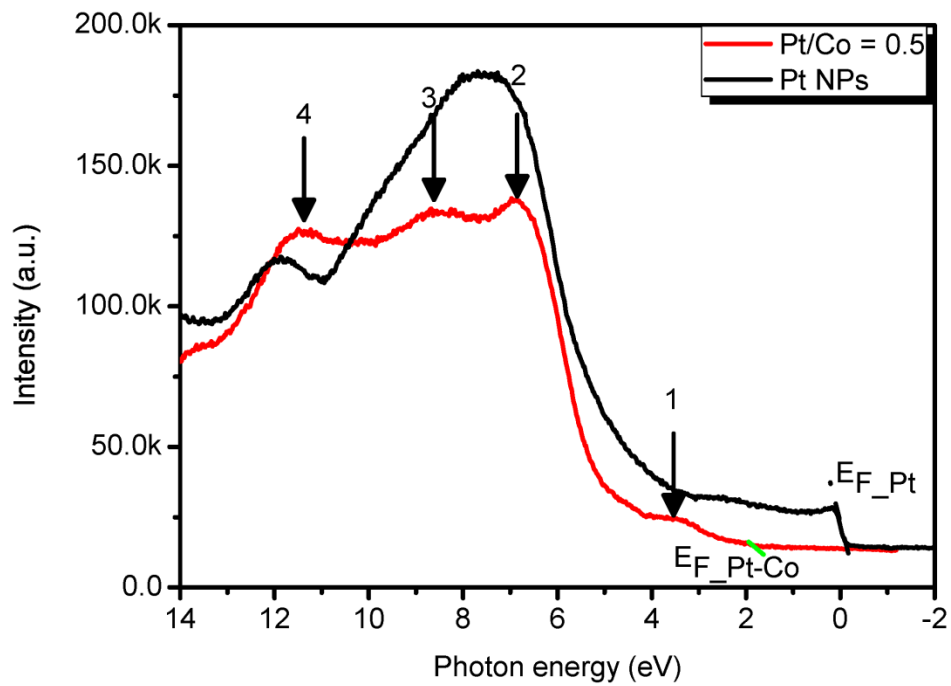
138 Table S3. EXAFS determined structure parameters of C/P CNCs of different Pt/Co
139 ratios.

CNCs	phase [*]	path	R	CN	σ^2	r factor
Pt/Co = 1.0	Co-C ^C	Co-C1	1.86	1	0.002	0.013
		Co-C2	1.95	1		
		Co-C3	2.11	1		
	Co ₃ O ₄	Co-O	1.99	3.1		
Pt/Co = 2.0	Co-C ^C	Co-C1	1.86	1.1	0.002	0.02
		Co-C2	1.95	1.1		
		Co-C3	2.11	1.1		
	Co ₃ O ₄	Co-O	1.99	3.3		
Pt/Co = 3.0	Co-C ^C	Co-C1	1.88	1.2	0.002	0.011
		Co-C2	1.97	1.2		
		Co-C3	2.13	1.2		
	Co ₃ O ₄	Co-O	2.01	2.6		

140 * Co-C^C: crystalline cobalt carbide including CoC₂, CoC₈, and Co₂(CO)₈.

141

142 5. UPS characterization



143
144 Figure S5. VB spectrum of C/P CNCs capping with uncompleted Pt shell (Pt/Co =
145 0.5).
146